Vortex pairs in viscoelastic Couette-Taylor flow

Matthias Lange[1,2] and Bruno Eckhardt[1]
[1]*Fachbereich Physik, Philipps Universität Marburg, D-35032 Marburg, Germany*
[2]*Fachbereich Physik, Carl von Ossietzky Universität, D-26111 Oldenburg, Germany*
(Received 15 May 2000; revised manuscript received 11 April 2001; published 10 July 2001)

In experiments on dilute polymers between rotating cylinders Groisman and Steinberg [Phys. Rev. Lett. **78**, 1460 (1997)] observed the formation of vortices that were not equidistantly spaced but rather paired up in what they called ''diwhirls.'' We calculate these states within an Oldroyd-B model with parameters adapted to the experiment and find good agreement with the observed characteristics of the diwhirls.

DOI: 10.1103/PhysRevE.64.027301 PACS number(s): 47.54.+r, 47.50.+d, 47.20.−k

Small amounts of polymers added to a fluid can change the large scale flow behavior in surprising and unexpected ways, ranging from rod climbing in laminar vortex flow to drag reduction in fully developed turbulent shear flows [1–4]. Some of these phenomena are fairly well understood, but others, in particular those involving more complicated flows, still await explanation. On the route from simple laminar flows to progressively more complicated flow topologies the Couette-Taylor cell stands out as a system particularly well suited for experimental and theoretical investigations. The flow between concentric cylinders is a closed shear flow that has a rich bifurcation structure with many different flow regimes already in the Newtonian case [5–7]. Interestingly, in the limit of large radii it goes over into plane Couette flow and some of the structures observed in curved Couette flow survive in this limit [8,9]. A number of studies have been devoted to various aspects of this viscoelastic Couette-Taylor problem (e.g., [10–15] and the review [4]).

A systematic study of the phase diagram of this system for a variety of polymer parameters was taken up recently by Groisman and Steinberg [16–20]. Using a special combination of polymer and solvent they could scan a large range of parameters, almost from the Newtonian limit to the extremely elastic limit. In particular, they observed a state of highly localized vortex pairs that they called diwhirls [17]. While there have been earlier observations of such states, then named ''tall Taylor cells'' [10], they apparently have not been studied theoretically. It is our aim here to analyze their properties in an Oldroyd-B model [2] with parameters adapted to the experiments at the Weizmann Institute.

Groisman and Steinberg [20] give an extensive discussion of the physical forces and rheological properties that can explain the elastic effects on the flow and the formation of diwhirls. In a Newtonian fluid Taylor vortices form as a centrifugal instability of the purely azimuthal Couette flow. Polymers can drive an instability through their elastic properties, by a mechanism similar to the one that gives rise to the Weissenberg effect [1]. This effect, usually demonstrated with a rotating rod, is due to a combination of elasticity and curvature. The internal elasticity of the polymers opposes any stretching and leads in the case of curved streamlines to a force that is directed towards the center of curvature. This force should also influence the vortices within a Couette-Taylor system with its curved streamlines [15].

Within this picture and with the information on the properties of the fluids used by Groisman and Steinberg it seems reasonable to start from a model where the stress tensor is divided into two parts, one containing the Newtonian properties of the solvent and the other the viscoelastic properties of the polymer [2]. The Newtonian part is characterized by the usual shear viscosity η_s for the solvent. The polymer part is described by a Maxwell model with a single relaxation rate λ and a viscosity η_p. In most of the experiments η_p is small, $\eta_p/(\eta_s+\eta_p)=0.074$, and kept fixed. This then leaves a single polymer parameter, the relaxation rate λ.

The experiments by Groisman and Steinberg are in a geometry with fixed outer cylinder and rotating inner cylinder. With d the gap between the cylinders, R_i and Ω_i the radius and rotation frequency of the inner cylinder, respectively, and ρ the density of the fluid, we can form a Reynolds number $\mathrm{Re}=R_i\Omega_i d\rho/\eta$, where $\eta=\eta_s+\eta_p$ is the total viscosity of polymer and solvent. The relaxation rate λ is made dimensionless by the advective time, giving the Deborah number $\mathrm{De}=\lambda R_i\Omega_i/d$. We denote the ratio between Deborah number and Reynolds number by $\kappa=\mathrm{De}/\mathrm{Re}$.

The equations of motion are given by

$$\partial_t\vec{u}=-(\vec{u}\cdot\vec{\nabla})\vec{u}-\frac{1}{\rho}\vec{\nabla}p+\frac{1}{\rho}\vec{\nabla}\cdot\tau, \tag{1}$$

where p is the hydrodynamic pressure and τ the stress tensor. The stress tensor τ has two contributions [2],

$$\tau=\tau_s+\tau_p, \tag{2}$$

which differ in their relation to the strain tensor $S=\vec{\nabla}\vec{u}+(\vec{\nabla}\vec{u})^T$. For the Newtonian solvent, $\tau_s=\eta_s S$. For the polymeric part, we take the constitutive equation

$$\tau_p+\lambda\frac{D\tau_p}{Dt}=\eta_p S, \tag{3}$$

with the upper convected derivative as time derivative,

$$\frac{D\tau_p}{Dt}=\partial_t\tau_p+(\vec{u}\vec{\nabla})\tau_p-[\tau_p(\vec{\nabla}\vec{u})^t+(\vec{\nabla}\vec{u})\tau_p]. \tag{4}$$

Of course, the flow is incompressible, $\vec{\nabla}\cdot\vec{u}=0$. Equations (1)–(4) define the Oldroyd-B model.

In all the numerical simulations and the stability analyses the flow was constrained to be axially symmetric. This limits the extent to which time-dependent studies can be compared with experiment but the axially symmetric diwhirls, the main aim of this work, are covered.

For the full numerical simulations the equations are discretized on a staggered grid [21,22] where the positions of

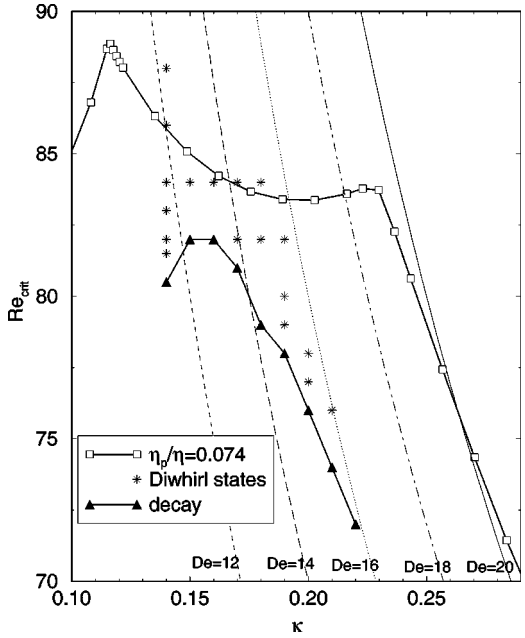

FIG. 1. Stability diagram in κ-Re space. The squares indicate the linear stability border between Couette flow and an oscillatory secondary flow. The stars refer to stationary diwhirl states obtained from a finite perturbation. The triangles represent decaying diwhirls, so that below this line the Couette flow is globaly stable. The dashed lines are lines of constant De.

velocity points and pressure points are shifted by half a grid size in order to avoid oscillatory solutions. Centered differences for the derivatives provide second order accuracy. A semi-implicit Crank-Nicholson scheme with iterative solution of the nonlinear equations was used for time integration [21]. Since Eq. (3) is of first order in the derivatives, an additional term $\beta\nabla^2\tau$ was added in order to suppress oscillatory numerical instabilities. This artificial viscosity dampens wavelengths of the order of the grid size and has only a neglible effect on the flow structures that typically extend over several grid points.

The calculations were carried out for a system with $\eta_p/\eta=0.074$ and $R_i/R_o=0.708$, where $\eta=\eta_s+\eta_p$ is the total viscosity of the solution and R_o the radius of the outer cylinder, in correspondence with the experiment [16]. The resolution of the spatial grid was 26 points in radial direction and 200 points in axial direction. This corresponds to a cylinder height of $8d$. We used periodic boundary conditions in axial direction. The calculations were started with Couette flow plus a disturbance of varying amplitude at fixed parameters Re and κ.

The radially symmetric Couette profile is not affected by the polymers and remains in the laminar flow state. Its stability properties, however, are changed. Following the method of Kupferman [13] we represent the linearized equations on a grid and study the resulting generalized eigenvalue problem. For the values of the experimental apparatus and the ratio $\eta_p/\eta=0.074$, we obtain the stability boundary shown in Fig. 1. There are three regions, separated by cusps in the stability border (upper curve). In each region a different state is formed in the bifurcation: Taylor vortex flow (TVF) for small $\kappa<0.11$, or oscillatory states for larger κ, but of two different wave numbers. These oscillating states have been found before in numerical studies of viscoelastic Couette-Taylor flow with an axial symmetry [12,23,24].

In agreement with the experiments [16], the critical Reynolds number is a bit lower than the Newtonian one, $\mathrm{Re}_{cr,N}=81.0$, for $\kappa<0.1$. The rapid drop in critical Reynolds number for $\kappa>0.23$ agrees with the experimental data, too, but the numerical simulations show a transition to an ordered oscillation, whereas the experiment shows disordered oscillations, presumably due to three-dimensional (3D) instabilities. As elasticity becomes more important the critical wave number increases considerably. In the intermediate region the 2D stability curve and the type of transition are very different from the experimental observations. This issue is perhaps related to the 3D instabilities that were observed in the calculations of Sureshkumar *et al.* [25] on a pure Maxwell fluid.

However, in the experiment axially symmetric structures emerge out of the three-dimensional flow as the Reynolds number is lowered. These states are best characterized as pairs of counter-rotating vortices with a narrow distance between their centers of vorticity and a larger spacing between the pairs. The interaction between the pairs is weak and the spacing between them is fairly irregular. When they first appear they oscillate relative to each other but become stationary as Re is further decreased. These stationary vortex pairs are the diwhirls [17]. They are axisymmetric and should be accessible to numerical study in our 2D model even though they arise out of a nonaxisymmetric flow.

Since the bifurcation to the formation of diwhirls is obviously subcritical we adopt in our numerical simulations the experimental protocol by first raising the Reynolds number above the stability line and then lowering it slowly. The experiments show that the intermediate state is 3D so that the formation of diwhirls as observed in the 2D simulation is not physically relevant. But as in the experiments the diwhirls persist below the linear instability line: the transition is strongly subcritical. Figure 1 shows the stability diagram in the κ-Re plane. All the stable and the decaying states were obtained by direct numerical simulation of the full equations and following the time evolution until the diwhirls either stabilized or decayed.

The actual shape of the diwhirls is compared to ordinary TVF in Fig. 2. While in TVF the vortices are almost symmetric, the diwhirls show a strong asymmetry between inflow and outflow. The region where fluid moves towards the inner cylinder (on the left-hand-side of the frame) is rather small and has a size of about $0.7d$. The outflow region increases in width from $2.0d$ at $\kappa=0.15$ to $2.4d$ at $\kappa=0.18$. The numbers quoted in [17] are an inflow region of $0.5d$ and an outflow region of $2.5d$.

Groisman and Steinberg [17–20] have characterized the vortices by the radial velocity measured along the middle of the cell in axial direction and by the axial velocity profile near the inner cylinder. Results from our simulation are shown in Figs. 3 and 4. From Fig. 3 of [19] one can read off a ratio of maximal ouflow velocity to maximal inflow velocity of about $0.7/5.5\approx0.13$ for states with various elasticities in a system with different geometry and different ratio η_p/η.

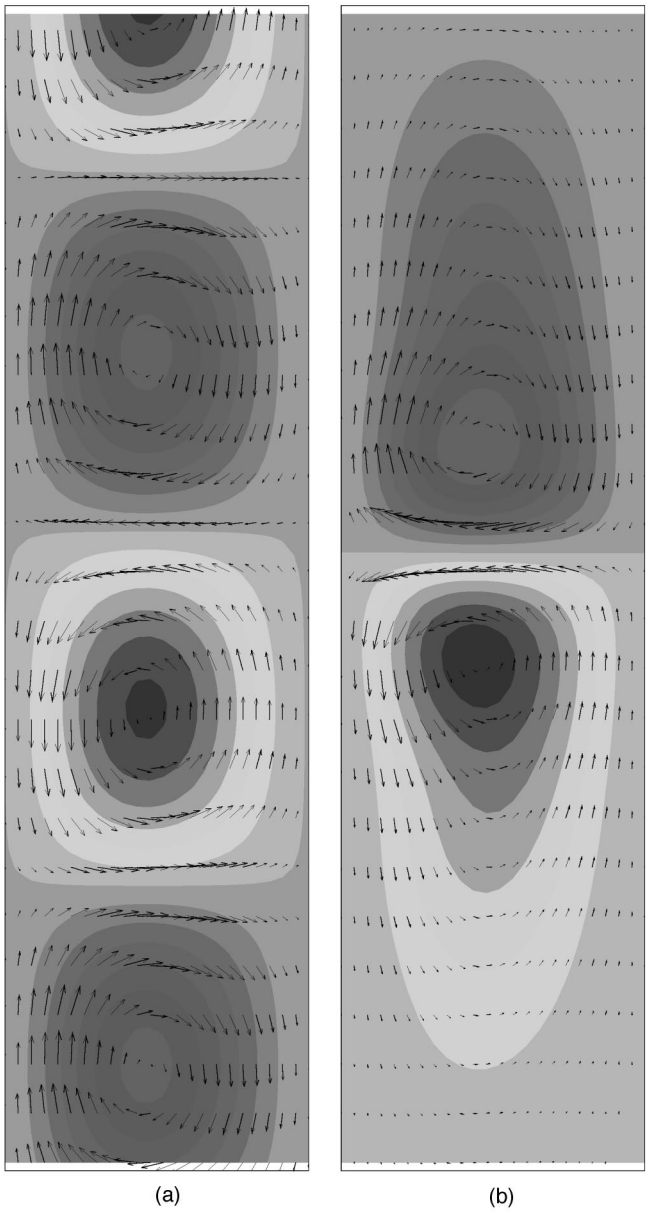

FIG. 2. Comparison between a typical vortex pair in TVF (a) and a diwhirl (b) visualized by the streamfunction. The latter shows a strong asymmetry between inflow and outflow, the inflow being concentrated in a very small region between the vortices. The inner cylinder is on the left-hand-side.

For our simulation Fig. 3 gives the ratio of about 0.2 with a strong dependence on κ. The distance between maximum and minimum is about $0.6d$ compared to the experimental $0.4d$. The flow structures are rather stable and not much affected by variations in κ and Re. Increasing the elasticity reduces the maximal outflow and smooths the oscillations in u_r. These spatial oscillations are an inertial effect, connected with the formation of small vortices at that distance. The modulations also appear in the axial velocity profiles (Fig. 4), which differ in this respect from the measured ones (Fig. 4 of [17]). The most likely explanation for the difference between our numerics and the experiments are the smaller values of Deborah number accessible in the numerics.

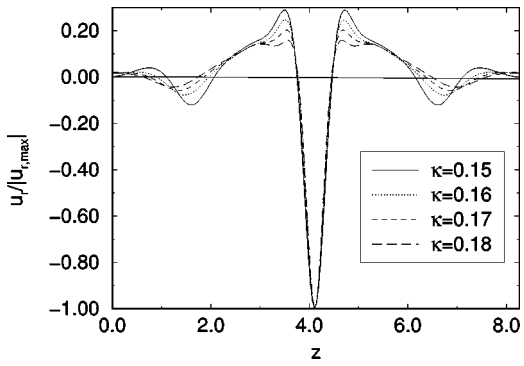

FIG. 3. Normalized diwhirl profiles u_r vs z for Re$=84.0$ and different κ. The strong inflow does not change with increasing elasticity and the size of the inflow region is about $0.7d$. The outflow increases with κ, from $2.0d$ at $\kappa=0.15$ to $2.4d$ at $\kappa=0.18$. The small vortices on both sides of the diwhirl are inertial effects. z is measured in gap sizes d.

Within the full numerical simulations we can also study the time evolution of the system. In the intermediate elasticity region that is numerically accessible here the interaction between the diwhirls is still noticeable. This is particularly clear from the sequence shown in Fig. 5, where a simulation is started with an initial condition that would evolve into the Taylor vortex state in the Newtonian case. Soon slight differences between the vortices are amplified and one vortex disappears. The weakening of a second vortex and its final disappearance is shown in a set of frames in Fig. 5. The state with three vortices does not change much as the integration continues. Lowering the Reynolds number a little bit and following the time evolution more than three times as long as for the previous sequence finally produces a state with three symmetrically placed diwhirls. This state then looks very much like the tall Taylor vortices observed by Beavers and Joseph in a polyacrylamid solution [10].

The favorable comparison between the experimental and numerical characterization of the diwhirls suggests that the Oldroyd-B model should provide a good starting point for an exploration of the full phase diagram [19,20], at least for intermediate elasticity. For higher elasticity parameters the

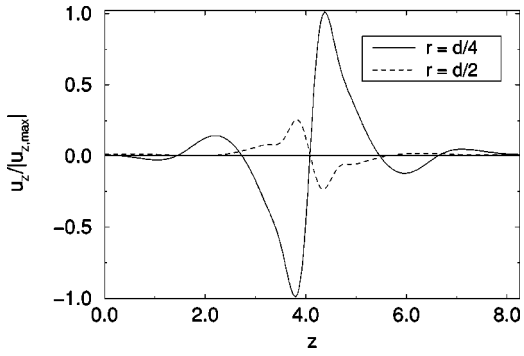

FIG. 4. Axial velocity profiles u_z vs z for Re$=81.0$ and $\kappa=0.14$ at distances of one-quarter and one-half gap width measured from the inner cylinder. The reversal in flow direction between the two profiles shows that the center of the vortices is not in the middle of the gap and that the profiles are taken on different sides of the center (this is already indicated by the vector field in Fig. 2). The maximum value for u_z in our units is 0.0139 for r=d/4 and 0.0034 for r=d/2.

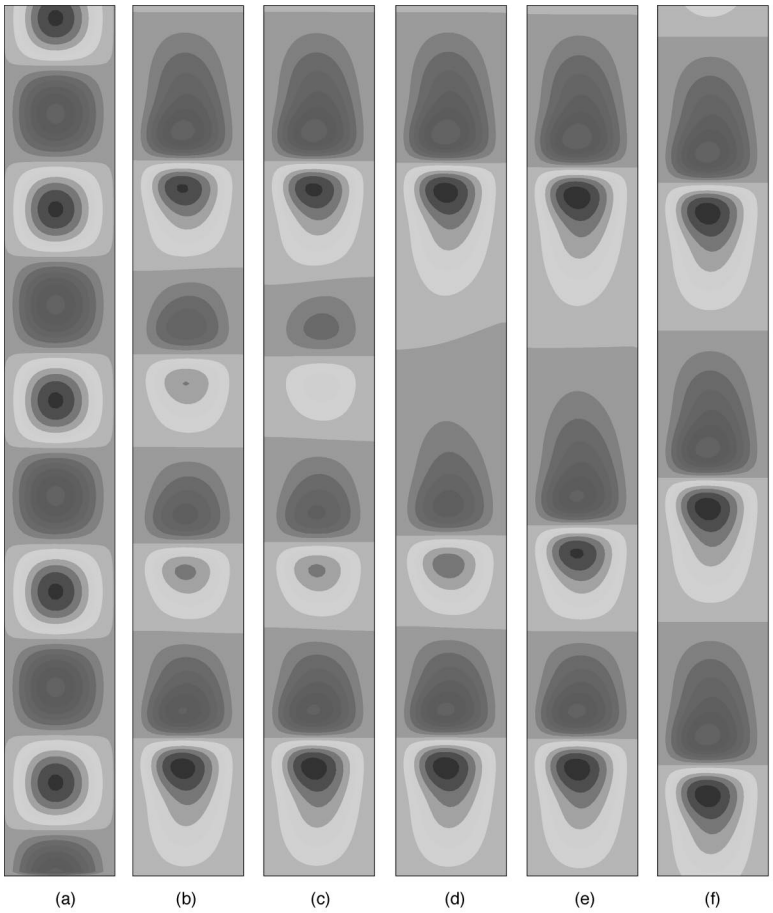

FIG. 5. Evolution of Taylor vortices into diwhirls visualized by the stream function. The parameters are $\kappa=0.15$, $\eta_p/\eta=0.074$, $\beta=0.0035$, and $L=8d$. The Reynolds number is $\mathrm{Re}=81.5$ for the first five frames and $\mathrm{Re}=80.0$ for the last one. The initial state (a) is an eigensolution of the linearized system. Within 600 time units four vortices of different strength have formed (b). The next two frames show the elimination of one more vortex at times 800 (c) and 1000 (d). Further rearrangements are slow, frame (e) being at time 1600. For the final frame, the Reynolds number was slightly lowered to $\mathrm{Re}=80.0$ and the system was integrated for another 5000 time steps. Frame (f) appears to be a stationary and symmetric arrangement of three diwhirls.

shear rates between the vortices increase considerably and nonlinear viscoelastic models have to be used (see, e.g., Kumar and Graham [26]).

We thank A. Groisman and V. Steinberg for many discussions on the experiment and M. Graham for pointing out the work of Beavers and Joseph. B.E. would like to thank the Institute for Theoretical Physics for the hospitality during the writing of the article. This work was supported in part by National Science Foundation under Grant No. PHY94-07194.

[1] K. Weissenberg, Nature (London) **159**, 310 (1947).
[2] R.B. Bird, C.F. Curtiss, R.C. Armstrong, and O. Hassager, *Dynamics of Polymeric Liquids* (Wiley, New York, 1987), Vol. 2.
[3] E.S.G. Shaqfeh, Annu. Rev. Fluid Mech. **28**, 129 (1996).
[4] R.G. Larson, Rheol. Acta **31**, 213 (1992).
[5] C.D. Andereck, S.S. Liu, and H.L. Swinney, J. Fluid Mech. **164**, 155 (1986).
[6] L. Koschmieder, *Bénard Cells and Taylor Vortices* (Cambridge University Press, Cambridge, England, 1993).
[7] R. Tagg, Nonlinear Sci. Today **4**, 1 (1994).
[8] M. Nagata, J. Fluid Mech. **217**, 519 (1990).
[9] H. Faisst and B. Eckhardt, Phys. Rev. E **61**, 7227 (2000).
[10] G.S. Beavers and D.D. Joseph, Phys. Fluids **17**, 650 (1974).
[11] B.J.A. Zielinska and Y. Demay, Phys. Rev. A **38**, 897 (1988).
[12] M. Avgousti and A.N. Beris, Proc. R. Soc. London, Ser. A**443**, 17 (1993).
[13] R. Kupferman, J. Comput. Phys. **147**, 22 (1998).
[14] M.K. Yi and C. Kim, J. Non-Newtonian Fluid Mech. **72**, 113 (1997).
[15] R.G. Larson, E.S.G. Shaqfeh, and S.J. Muller, J. Fluid Mech. **218**, 573 (1990).
[16] A. Groisman and V. Steinberg, Phys. Rev. Lett. **77**, 1480 (1996).
[17] A. Groisman and V. Steinberg, Phys. Rev. Lett. **78**, 1460 (1997).
[18] A. Groisman and V. Steinberg, Philos. Mag. B **78**, 253 (1998).
[19] A. Groisman and V. Steinberg, Europhys. Lett. **43**, 165 (1998).
[20] A. Groisman and V. Steinberg, Phys. Fluids **10**, 2451 (1998).
[21] R. Peyret and T.D. Taylor, *Computational Methods for Fluid Flow* (Springer-Verlag, New York, 1983).
[22] C.A.J. Fletcher, *Computational Techniques for Fluid Dynamics* (Springer-Verlag, Berlin, 1988), Vol. I.
[23] P.J. Northey, R.C. Armstrong, and R.A. Brown, J. Non-Newtonian Fluid Mech. **42**, 117 (1992).
[24] M. Avgousti, B. Liu, and A.N. Beris, Int. J. Numer. Methods Fluids **17**, 49 (1993).
[25] R. Sureshkumar, A.N. Beris, and M. Avgousti, Proc. R. Soc. London, Ser. A **447**, 135 (1994).
[26] K.A. Kumar and M.D. Graham, Phys. Rev. Lett. **85**, 4056 (2000).